Levels in ^{13}N examined by ^{12}C+p elastic resonance scattering with thick target *

QIN Xing(秦星)[1,2;1)] WANG You-Bao(王友宝)[1] BAI Xi-Xiang(白希祥)[1] GUO Bing(郭冰)[1]
JIANG Chao(蒋超)[1,2] LI Yun-Ju(李云居)[1,3] LI Zhi-Hong(李志宏)[1] LIAN Gang(连钢)[1]
SU Jun(苏俊)[1] WANG Bao-Xiang(王宝祥)[1] ZENG Sheng(曾晟)[1] LIU Wei-Ping(柳卫平)[1]

1 (Department of Nuclear Physics, China Institute of Atomic Energy, Beijing 102413, China)
2 (Institute of Modern Physics,Shanxi Normal University, Linfen 041004, China)
3 (Institute of Physical Engineering, Zhengzhou University, Zhengzhou 450052, China)

Abstract The elastic resonance scattering of ^{12}C+p has been studied in inverse kinematics via a novel thick target method at GIRAFFE facility of HI-13 tandem accelerator laboratory, Beijing. The recoil protons were measured by a ΔE-E counter telescope based on a large area double-sided silicon strip detector at laboratory angles around $\theta_0 = 15^\circ$. The excitation function for ^{12}C(p,p) elastic scattering has been obtained over a wide energy range of $E_{\rm c.m.}$=0.31—3.45 MeV, which was explained quite well by the R-matrix calculation with known resonance parameters of the first three levels in ^{13}N nucleus. Thus it is demonstrated that the present setup can be directly applied to the study of elastic resonance scattering with secondary radioactive beams.

Key words elastic resonance scattering, excitation function, thick-target method

PACS 21.10.Hw, 21.10.Jx, 25.40.Ny

1 Introduction

The conventional proton resonance scattering has been a powerful spectroscopic tool to explore the properties of compound nucleus levels close to the threshold, which are usually of astrophysical and structural significance. It is a kind of precise yet very time-consuming experiment, since one needs to change the proton beam energy in small steps in order to obtain an excitation function of the energy range in interest. To use radioactive ion beam with limited intensity and short lifetime, more efficient experimental method with the emphasis of inverse kinematics must be employed. For this purpose, the thick target method has been proposed and rapidly applied[1—3]. It uses an either solid or gas target containing hydrogen atoms with thickness enough to stop the incident beam or degrade its energy to the region of interest. By measuring the lighter recoil particles at laboratory forward angles, one can rebuild the reaction kinematics taking account of the energy losses of particles in the target. By using this method, one can study several resonances simultaneously with a single bombarding energy of exotic beam.

The method provides a way to efficiently measure an excitation function with a one-shot experiment, however, the complicity here is that at any individual angle, the proton energy spectrum is continuous over a certain range corresponding to the energy losses of particles in the thick target, therefore the detector system must have satisfactory angular resolution as the primary requirement, in order to retain the accuracy when dealing with proton events from different angles. Prior to this work, a ΔE-E counter telescope has been developed consisting of detectors with large acceptance and high granularity. The setup was initially tested with ^{17}F+p elastic resonance scattering[4]. Besides the problem of deficient ^{17}F beam intensity, the geometry with detectors at 0° used in the ^{17}F+p testing runs was found particularly inadequate due to the malfunction of the detectors caused by the leaked higher-energy contaminants

Received 5 March 2008

* Supported by National Natural Science Foundation of China (10445004, 10575136, 10735100) and Major State Basic Research Development Program (2007CB815003)

1) E-mail: qinxing0917@163.com

in the secondary beam. With an improved setup and much enhanced ^{13}N secondary beam intensity, the ^{13}N+p elastic resonance scattering was recently studied[5] at the secondary beam facility[6, 7] of HI-13 Tandem laboratory. For a cross check of the thick-target method and the performance of detector system, the ^{12}C+p elastic resonance scattering was studied successively as a part of the ^{13}N+p scattering experiment.

2 Experiment

The ^{12}C+p scattering experiment shared the same setup to that for ^{13}N+p. During the first part of experiment, the ^{13}N ions were produced by the ^{2}H(^{12}C, ^{13}N)n reaction. The front end of the secondary beam facility consists of a deuteron gas target covered by Havar foils. The ^{13}N ions were selected and focused by a dipole and a quadruple doublet magnets, and were further purified by a Wien velocity filter[8, 9]. To restrict the spot size of secondary beam on the target, a collimator complex consisting of two apertures of $\phi 9$ and $\phi 5$ mm in diameter was used. The back end detector system installed inside the reaction chamber is shown in Fig. 1.

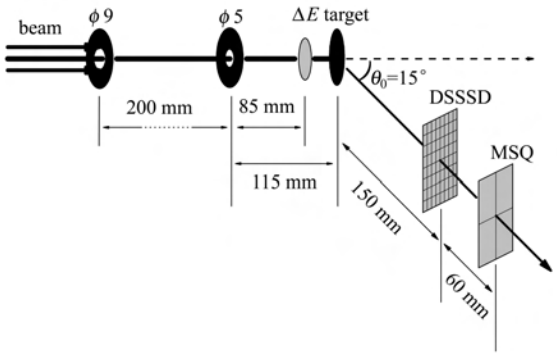

Fig. 1. Scheme of the experimental setup.

In the second part of the experiment for ^{1}H(^{12}C,p) runs, the gas cell was pumped empty, the ^{12}C incident beam initially of 60 MeV was scattered by the Havar foils into the secondary beam line. After passing through the same transport system, the ^{12}C beam was collimated by the collimator complex and monitored by a 13.2 μm-thin ΔE detector. The role of the ΔE detector was to record the beam for normalization. The energy of the ^{12}C beam after the ΔE detector was (46.3±1.1) MeV, the intensity was about 1.2×10^4 particles/s. A foil of polyethylene $(CH_2)_n$ with a thickness of 9.33 mg/cm^2 was used as the reaction target, its thickness is enough to fully stop the ^{12}C particles. Separate runs with a 10.88 mg/cm^2-thick pure carbon target were also taken to evaluate the background originated from the carbon atoms in the $(CH_2)_n$ target.

The recoil protons from the ^{1}H(^{12}C,p) reaction were detected by a ΔE-E telescope, which consists of a 63 μm-thick Double-Sided Silicon Strip Detector (DSSSD)[10, 11] and a 982 μm-thick quadrant Multi-guard Silicon Quadrant (MSQ) detector. Both detectors have the same sensitive area of 50 mm×50 mm. The DSSSD is position sensitive with a resolution of 3 mm×3 mm. The ΔE-E telescope was placed at laboratory angle of $\theta_0 = 15^\circ$. In this geometry, the $\theta_{\rm lab}$ of each 3 mm×3 mm pixel of the DSSSD can be evaluated by

$$\theta_{\rm lab} = \arccos\left(\frac{d_0\cos\theta_0 \pm x\sin\theta_0}{\sqrt{d_0^2+x^2+y^2}}\right), \qquad (1)$$

where d_0 refers to the distance between the centers of the target and the DSSSD, i.e., 150 mm; x, y are the coordinates in the plane of the DSSSD if setting the origin at its center. Due to the limitation of the available data acquisition system, only the inner half of the DSSSD area was used while the outer part was blocked. It covered a range of $\theta_{\rm lab}$=10°—20°, corresponding to $\theta_{\rm c.m.}$=180° − 2$\theta_{\rm lab}$=140°—160° in the center of mass frame.

The calibration of the recoil proton spectrum was made by using proton beam scattering on Au of 440 μg/cm^2 at several energies and by using a standard ^{239}Pu and ^{241}Am mixed alpha source. The scatter plot of ΔE-$E_{\rm t}$ after the calibration is shown in Fig. 2 as a sum of available pixels. The α particles in Fig. 2 were probably generated from the ^{12}C(^{12}C,α)^{20}Ne reaction.

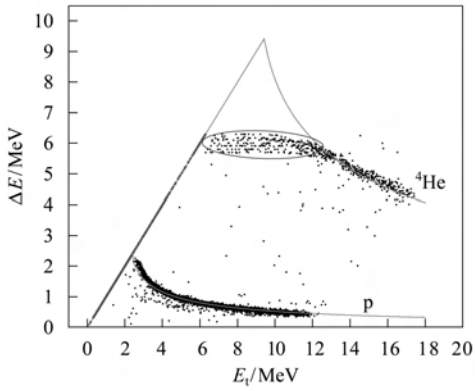

Fig. 2. The scatter plot of ΔE-$E_{\rm t}$ measured with the DSSSD and MSQ detectors. The solid lines show the results of the energy loss calculation. The circled α events were due to the energy losses in the DSSSD overflowing the dynamic range of the amplifier.

3 Analysis

3.1 Data analysis

The detected proton total energy E_t can be converted into $E_{c.m.}$ at each angle according to

$$E_{c.m.} = E_p \times \frac{m_p + m_C}{4m_C \cos^2\theta_{lab}}, \quad (2)$$

in the formula, m_C and m_p are the masses of carbon and proton, respectively, E_p refers to the proton energy at the reaction point which can be obtained by adding E_t and the proton energy loss ΔE_p in the $(CH_2)_n$ target. To retrieve ΔE_p, a Monte Carlo program was developed combining the reaction kinematics with the energy loss of ^{12}C and proton in the $(CH_2)_n$ target according to each θ_{lab}. As an example, a simulated $E_{c.m.}$ versus E_t for a pixel centered at $\theta_{lab} = 12^\circ$ is shown in Fig. 3. In the simulation, the ^{12}C beam energy was taken as (46.3±1.1) MeV, the θ_{lab} resolution as $\Delta\theta_{lab} = 0.8^\circ$, the latter was evaluated by considering the beam angular divergence, the beam spot, and the coverage of each pixel in the DSSSD. In the course of E_p to $E_{c.m.}$ conversion, the uncertainty of $E_{c.m.}$ was estimated to be ±20 keV mainly due to the θ_{lab} resolution and the energy straggling of particles in the target.

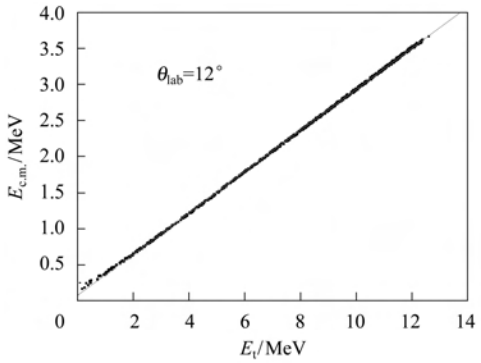

Fig. 3. The simulated $E_{c.m.}$ versus the detected proton total energy E_t for a pixel centered at $\theta_{lab} = 12^\circ$. The simulated date were fitted with a linear function to obtain the relation between $E_{c.m.}$ and E_t, as shown in the solid line.

The proton yield after the E_p to $E_{c.m.}$ conversion were added up over different pixels, the higher-energy part of the summed experimental proton yield is shown in Fig. 4 together with that from the carbon target. As is shown in Fig. 4, the proton yield with the carbon target is rather flat without any sharp structure while the one from the $(CH_2)_n$ target has clear peak at $E_{c.m.} \approx 1.6$ MeV. The proton events in the range of $E_{c.m.}$=0.31—0.68 MeV were not included in Fig. 4. These protons had E_t <2.5 MeV, therefore were stopped solely in the DSSSD. Fortunately, these protons can be resolved by applying criterions of E_t <2.5 MeV plus energy loss in the MSQ as zero.

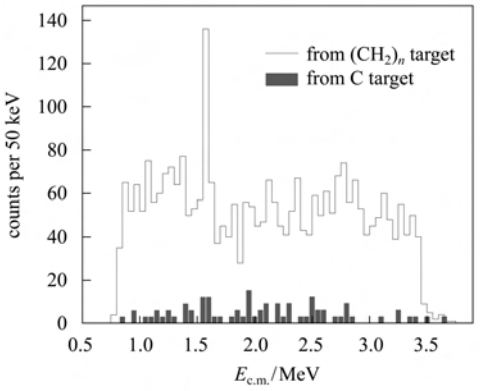

Fig. 4. The proton yield after E_p to $E_{c.m.}$ conversion together with that from the carbon target.

The proton events from the carbon target were normalized to those from the $(CH_2)_n$ target, by the total number of incident ^{12}C ions and by the effective target thickness of per $E_{c.m.}$ unit. The latter was done by computing the number of carbon atoms corresponding to the range difference between the maximum and the minimum energies of per $E_{c.m.}$ unit in $(CH_2)_n$ and carbon, respectively. After normalization, the proton yield with the carbon target was about 1/13 of that with the $(CH_2)_n$ target. The net proton yields from the ^{12}C+p scattering were obtained after background subtraction. The averaged differential cross sections were then deduced from the net proton yields according to

$$\frac{dN'}{dE} = I_{beam}\frac{dN_s}{dE}\frac{d\sigma}{d\Omega}d\Omega, \quad (3)$$

where $dE = E_2 - E_1$ refers to per $E_{c.m.}$ unit, I_{beam} is the number of incident ^{12}C, dN_s/dE the energy dependent hydrogen atom number. The dN_s/dE was calculated by the ^{12}C range difference between the maximum and the minimum energies of per $E_{c.m.}$ unit, as aforementioned. Moreover, it was also checked by a Monte Carlo simulation of the target depth versus $E_{c.m.}$ where the scattering taking place, as shown in Fig. 5. The two methods agreed well within errors of less than 1%. The averaged $d\sigma/d\Omega$ in the center of mass frame was then deduced by

$$\left(\frac{d\sigma}{d\Omega}\right)_{c.m.} = \frac{1}{4\cos\theta_0}\left(\frac{d\sigma}{d\Omega}\right)_{lab}, \quad (4)$$

where $\theta_0 = 15^\circ$.

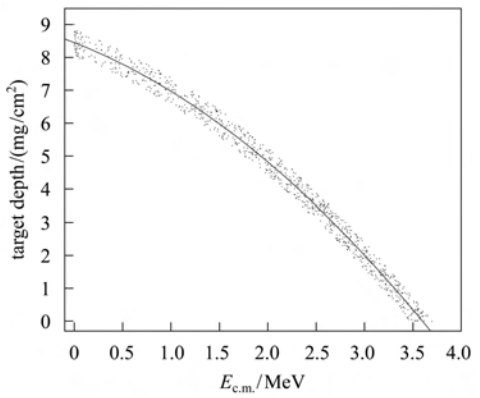

Fig. 5. A Monte Carlo simulation of the target depth vs $E_{c.m.}$ where the scattering takes place. The simulated data were fitted with a two-order polynomial function to obtain the relation which is angle independent. The effective target thickness of per $E_{c.m.}$ unit was then the corresponding depth difference in the vertical axis.

3.2 *R*-matrix analysis

The conventional formalism to solve the resonant process is *R*-matrix theory[12]. A resonance state, if it exists with a sufficiently large width, can be identified in the excitation function as an interference pattern of potential and resonance scattering. The resonance energy, width and J^π can be determined from the *R*-matrix fitting calculation of the excitation function. The general assumption of *R*-matrix theory is that for every reaction channel, there exists a channel radius a_c and the resonance can take place only in the internal region. a_c is normally presented as

$$a_c = r_0(A_p^{1/3} + A_t^{1/3}), \tag{5}$$

where A_p and A_t are the projectile and target mass numbers, r_0 is the unit radius independent of A_p and A_t. In the inner region, the *R*-matrix element is expressed in a simple form of

$$R_{c'c} = \sum_\lambda \frac{\gamma_{\lambda c}\gamma_{\lambda c'}}{E_\lambda - E}\ , \tag{6}$$

where λ labels the members of a complete set of states, $\gamma_{\lambda c}$ is the reduced-width amplitude, E_λ the energy eigenvalues of the states λ.

4 Results

The experimental excitation function of the ^{12}C+p scattering is shown in Fig. 6. The error bars indicate statistical uncertainty only. The systematical errors including the uncertainties in the detector solid angle and beam normalization were small and negligible comparing with the statistical error. Since the proton threshold in ^{13}N is of 1.9435 MeV[13], the excitation energy in ^{13}N is simply $E_x = E_{c.m.} + 1.9435$ MeV. The first three levels in ^{13}N were revealed in the excitation function, which are all above the proton threshold. Two peaks are prominent at $E_{c.m.} \approx 0.42$ and ≈ 1.61 MeV, corresponding to the 2.36 MeV $1/2^+$ and 3.55 MeV $5/2^+$ states in ^{13}N, respectively. A small dip can be seen at $E_{c.m.} \approx 1.56$ MeV, which is due to the $3/2^-$ level at 3.50 MeV.

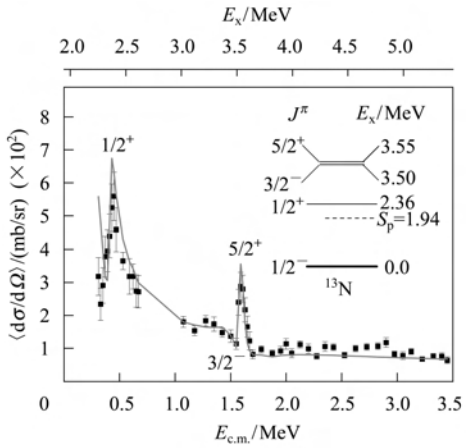

Fig. 6. Experimental excitation function for the ^{12}C+p elastic resonance scattering, the *R*-matrix fitting calculation is shown as the solid line. The gap between $E_{c.m.}$ =0.7 and 1.0 MeV was due to the detector dead layers.

The fitting calculation was done with a multilevel *R*-matrix code MULTI7.0[14]. The inelastic scattering process can be excluded because the $E_{c.m.}$ needs to be greater than 4.44 MeV to populate the first excited state of ^{12}C. Since the ground state of ^{12}C has a spin and parity of 0^+, the $^{12}C_{g.s.}$+p scattering channel spin is simply $s = 1/2^+$. For each resonance state, the proton is assumed to decay from a single-particle orbital of l_j, in this picture, the first three levels in ^{13}N correspond to $2s_{1/2}$, $1p_{3/2}$ and $1d_{5/2}$, respectively. l = 0, 1 and 2 were therefore used for the conservation of total angular momentum. The input widths of $\Gamma_R = 31.7$, 62 and 47 keV for these there levels are from the compiled values[13]. The channel radius used for the resonances and the hard-sphere scattering is 4.6 fm according to Eq. (5). One can see that the theoretical curve agrees well with the experimental excitation function, indicating that the experimental excitation function can be well reproduced with the known resonance energies.

5 Summary

In summary, the elastic resonance scattering of ^{12}C+p has been investigated via a novel thick-target method. The experimental setup used in this work was intent to imitate the situation of radioactive

secondary beam. The first three levels in ^{13}N were clearly identified in the experimental excitation function. The deduced resonance parameters agree well with the compiled values, which demonstrates that the setup can be applied to measuring the elastic resonance scattering induced by the currently available radioactive secondary beams at the HI-13 tandem accelerator laboratory.

The authors thank Professor John Shriner at Tennessee Tech University for providing us the multi-level R-matrix code MULTI7.0. We would like also to thank the technical staff of the HI-13 tandem accelerator laboratory for preparing the targets and operating the machine carefully.

References

1 Markenroth K, Axelsson L, Baxter S et al. Phys. Rev. C, 2000, **62**: 034308
2 Kubono S. Nucl. Phys. A, 2001, **693**: 221
3 Smith M S, Rehm K E. Annu. Rev. Nucl. Part. Sci., 2001, **51**: 91
4 WANG You-Bao, WANG Bao-Xiang, BAI Xi-Xiang et al. HEP & NP, 2006, **30**(Suppl. Ⅱ): 202 (in Chinese)
5 WANG Y B, WANG B X, QIN X et al. Phys. Rev. C, 2008, **77**: 044304
6 BAI Xi-Xiang, LIU Wei-Ping, QIN Jiu-Chang et al. Nucl. Phys. A, 1995, **588**: 273c
7 LIU Wei-Ping, LI Zhi-Hong, BAI Xi-Xiang et al. Nucl. Instrum. Methods. Phys. Res. B, 2003, **204**: 62
8 LI Zhi-Hong, LIU Wei-Ping, BAI Xi-Xiang et al. HEP & NP, 2006, **30**(Suppl. Ⅱ): 258 (in Chinese)
9 ZENG Sheng, LI Zhi-Hong, LI Gang et al. Atomic Energy Science and Technology, 2007, **41**: 513 (in Chinese)
10 Bergmann U C, Fynbo H O U, Tengblad O. Nucl. Instrum. Methods Phys. Res. A, 2003, **515**: 657
11 Tengblad O, Bergmann U C, Fraile L M et al. Nucl. Instrum. Methods A, 2004, **525**: 458
12 Lane A M, Thomas R G. Rev. Mod. Phys., 1958, **30**: 257
13 Ajzenberg-Selove F. Nucl. Phys. A, 1991, **523**: 1
14 Nelson R O, Bilpuch E G, Mitchell G E. Nucl. Instrum. Methods Phys. Res. A, 1985, **236**: 128